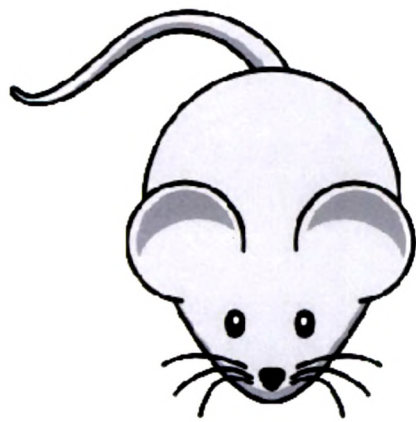
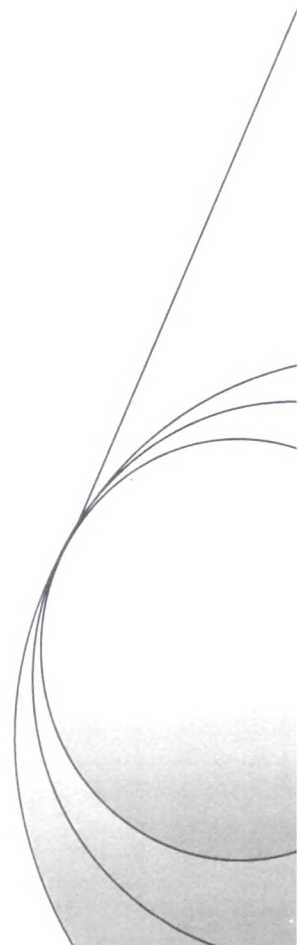
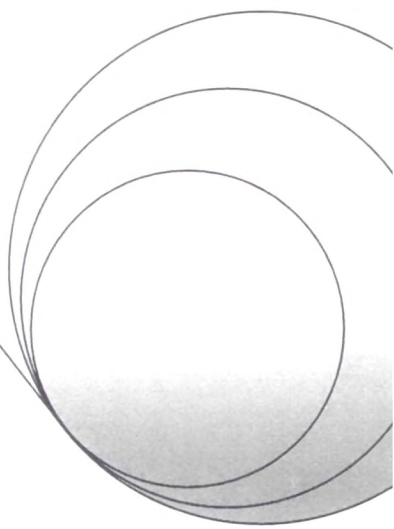


Chapter 7



In Vivo STUDIES ON NANOPARTICLES



7. In-Vivo STUDIES ON NANOPARTICLES

7.1 Introduction

7.1.1 Radiolabeling and biodistribution:

Radiolabeling of drugs and drug delivery systems has been widely applied to study the biodistribution patterns. Particularly, the radiolabeling with short-lived radionuclides has been preferred due to their rapid decay and hence low toxicity. The compounds are linked to radionuclides that are prepared in a way to concentrate by a particular organ or physiological process. In a typical radiopharmaceutical formulation, the quantity of radionuclide used is quite small. In general, the radiopharmaceuticals differ from the conventional pharmaceuticals in that it is not intended to elicit a pharmacological response. Consequently the radiopharmaceuticals do not disturb the physiological process being measured, function as true tracer and are usually free from hypersensitivity reactions.

The ability of radiopharmaceuticals to function as indicators of specific physiologic processes provide an important measure of disease that might not appear on the basis of structural changes alone. Such functional measurements provide a powerful diagnostic tool. Radiopharmaceuticals share with conventional parenteral drugs in their requirements of purity and efficacy. The formulation of a radiopharmaceutical is more complex. The decay process may result in change in final radionuclide composition and in the degradation of the stable materials. Variation in quality of radiopharmaceutical can greatly affect the biodistribution pattern and thereby the ultimate scan quality, causing problems in interpretation.

The pathway of an internally administered radioisotope having favourable nuclear characteristics could be traced noninvasively with an external detection system like gamma camera (Single Photon Emission Computed Tomography). Single Photon Emission Computed Tomographic imaging represents methods for acquiring and processing the scintigraphic data to reconstruct a three dimensional tomographic image displaying the distribution of radioactivity within certain organ system using emitted gamma rays upon administration of a radio tracer (Budinger, 1980, Sorensen and Phelps, 1980). This led to an increased demand for short-lived radionuclides which could be safely administered in larger doses resulting in excellent image quality.

For biological experimentation, the radionuclides are linked to the compounds of interest by various techniques. The effective binding of radiolabel to the compound is determined by quality control tests such as labelling efficiency and stability of complexes in serum.

In practice, the radiopharmaceutical preparation is administered to the species of interest, usually by parental route. At specified time intervals, the organs or tissues of interest was isolated and measured for radioactivity using gamma counter. The images of organs/tissues can also be taken without sacrificing the host using the gamma camera.

Various radionuclides are used for the above mentioned purposes include ^3H , ^{14}C , ^{32}P , ^{35}S , ^{99}Mo , ^{131}I , ^{123}I , ^{133}Xe , ^{201}Tl , $^{99\text{m}}\text{Tc}$, ^{67}Ga , ^{111}In (Ramamoorthy and Desai 1997).

$^{99\text{m}}\text{Tc}$ was widely used for the pharmacokinetic and biodistribution studies of drugs and drug delivery systems (Reddy et al., 2004; Subramanian et al., 2003; Seyed et al., 2010).

7.1.2 *In-vivo* studies for nanoparticles:

Many studies reported the application of nanoparticles in the improvement of bioavailability of poorly water soluble drugs, as sustained release carriers for parental administration, as active or passive targeted delivery systems, prevention of drug from the degradation, reduce toxicity or side effects by modifying their *in vivo* distribution (Kreuter, 1994).

Delivery of anticancer agents to tumors using colloidal delivery systems like nanoparticles with an objective of enhancement in tumor concentrations has been widely attempted. Melanoma model is used in various studies to ascertain the effectiveness of delivery systems.

Melanoma is the leading cause of death from cutaneous malignancies (Folkman, 1987). It has been suggested that the invasiveness of malignant tumor cell is due to their reduced adhesiveness. Malignant transformation could be associated with general enzymatic changes leading towards increased proteolytic and fibrinolytic activity in tumor cells. The significance of angiogenesis in tumor development and metastasis is well established and it was confirmed previously that a significant correlation exists between tumor angiogenesis and ability of melanoma to metastasize (Claffey et al., 1996). It was also reported that in murine melanoma model combination treatment with antiangiogenic agent and chemotherapeutic agent increased antitumor efficacy (Dabrowska-Iwanicka et al., 2002). Thus we performed experiments in metastatic murine melanoma tumor model to study tumor growth *in vivo*.

Additional studies were performed to evaluate the antiangiogenesis by determining the tumor microvessel density (MVD).

7.2 Radiolabeling:

7.2.1 Radiolabeling procedure:

The radiolabeling of free drug solutions ET and QD as well as ETN and QDN formulations were carried out using direct labeling procedure with technetium-99m ($^{99\text{m}}\text{Tc}$) by reducing

technetium of sodium pertechnetate in the presence of reducing agents like stannous chloride (Arulsudar et al., 2003).

Briefly, to 0.5 ml of nanoparticle formulations and free drug solutions, 1.0 ml of ^{99m}Tc in saline (upto 2 mCi/ml) was added followed by reduction with stannous chloride dihydrate ($\text{SnCl}_2 \cdot 2\text{H}_2\text{O}$) solution 1mg/ml. The pH was maintained at about 6.5-7 with 0.5 M Sodium bicarbonate. Then the mixtures were incubated at ambient temperature for definite time period. The amount of SnCl_2 (10, 25, 50 μg) and incubation time (15, 30, 45 min.) was optimized considering the labeling efficiency.

The results were depicted in Table 7.1.

7.2.2 Evaluation of radiolabeling efficiency:

The radiolabeling efficiency of free drug and nanoparticles is determined by ascending instant thin layer chromatography (ITLC) using acetone as mobile phase on Whatman 3 paper strips or silica gel-coated fiber sheets as stationary sheets.

Whatman 3 paper strips of 12 cm were cut, marked at 1cm interval. The radioactivity preparation to be evaluated was spotted and the strips were removed when solvent front reached around 10 cm, allowed to dry. The strip was cut at 1cm marking and the radioactivity in each segment was determined in a well type gamma ray counter (Sodium iodide scintillation counter, Electronics Corporation of India Ltd., Mumbai).

7.2.3 In-vitro serum stability of the ^{99m}Tc -labeled Complexes:

Stability of the ^{99m}Tc -labeled complexes of drugs and nanoparticles was determined in vitro in serum by ascending TLC technique at different time points ($\frac{1}{2}$, 2, 6, and 24 hrs.) as described in previous section. A volume of 100 μl of ^{99m}Tc complex solution was added to 1ml of fresh serum, and then this mixture at each time point was spotted to TLC strip, and the percentage of ^{99m}Tc complex was determined using the method described above (Table 7.2).

7.2.4 Tumor implantation:

The use of animal was as per the norms set by the Social Justice & Empowerment Committee for the purpose of control and supervision of experiments on animals (CPCSEA). Approval for animal experimental work was as per ethical committee of Jawaharlal Nehru Cancer Hospital (JNCH & RC), Bhopal, India.

C57BL/6 mice (male or female) of average age between 6-7 weeks old with average weight of 25 ± 3 gm were s.c. inoculated in the thigh region of right hind leg with 5×10^5 tumor cells B16F10 cells maintained *in vivo* in department of research (JNCH & RC). After 7-8 days, a palpable tumor in the volume range of 90- 100 mm^3 was observed near the site of injection.

7.2.5 Pharmacokinetic and Biodistribution Study:

Biodistribution studies of ^{99m}Tc -nanoparticle complexes were carried out according to the approved method by local animal ethical committee of JNCH and RC. C57BL/6 mice bearing desired size B16F10 tumor (~1 to 1.5 cm), were injected with 0.1 ml of ^{99m}Tc labelled complex (200 μCi of ^{99m}Tc) of ETN and QDN as well as ET and QD. Blood samples were collected from the retro-orbital plexus of mice eye at each time point (5, 15, 30, 60, 120, 240, 720, 1440 min) ($n = 3$ at each time point). The blood was weighed and the radioactivity present in the whole blood was calculated by keeping 7.3% of the body weight as the total blood weight (Wu et al., 1981). The results obtained are plotted as time Vs % injected dose as depicted in Figure 7.1.

The biodistribution studies are performed after 2 hours, 6 hours, and 24 hours postinjection ($n = 3$). At these time intervals, the blood is collected, the animals are sacrificed by cervical dislocation, and the major organs (heart, liver, spleen, kidney, lungs, tumor) were isolated. Before dissecting the animals, whole body images were taken using single photon emission computerized tomography gamma camera (Siemens, Germany) (Figure 7.4). The organs are then weighed and measured for radioactivity in gamma counter. The radioactivity is interpreted as percentage of injected dose per gram of organ/tissue (Table 7.3 and 7.4).

7.2.6 Gamma Scintigraphy:

^{99m}Tc -labeled complex of ETN and QDN containing 100 μCi of ^{99m}Tc is injected subcutaneously near the B16F10 tumor region in C57BL/6 mice. After 1 and 48 hour post injection, the mice was fixed on animal fixing tray board and imaging has to be performed with Single Photon Emission Computed Tomography Gamma Camera. The gamma images are presented in Figure 7.2 and 7.3 for ETN and QDN respectively.

Table 7.1 Optimized conditions for ^{99m}Tc -labelling

Parameters Optimized	ET	QD	ETN	QDN
Conc. Of SnCl_2 (μg)	25	50	50	50
Incubation time (min)	15	30	15	15
Maximum labeling efficiency achieved (%)	97.76	88.23	99.63	94.12

Table 7.2 *In vitro* serum stability of ^{99m}Tc -labeled complexes of ET, QD, ETN and QDN

Time in hrs.	Mean Labeling Efficiency (%)			
	ET	QD	ETN	QDN
1/2	97.50	88.23	99.51	93.60
2	98.23	86.84	97.70	91.96
6	95.48	84.52	95.07	90.17
24	88.07	77.14	94.76	88.04

n = 3

Table 7.3 % Injected dose of ^{99m}Tc -labeled complexes appearing in blood at various time points

Time in min.	Mean % Injected dose in blood of ^{99m}Tc complex			
	ET	QD	ETN	QDN
5	0.021±0.01	0.015±0.01	0.018±0.01	0.012±0.02
10	0.037±0.02	0.022±0.01	0.032±0.01	0.020±0.03
30	0.052±0.02	0.046±0.02	0.042±0.02	0.035±0.01
60	0.087±0.04	0.072±0.02	0.074±0.01	0.062±0.03
120	0.101±0.01	0.096±0.01	0.086±0.03	0.076±0.02
240	0.148±0.02	0.137±0.01	0.179±0.03	0.162±0.04
720	0.169±0.01	0.160±0.02	0.195±0.01	0.182±0.03
1440	0.110±0.01	0.105±0.01	0.143±0.01	0.138±0.01

n = 3

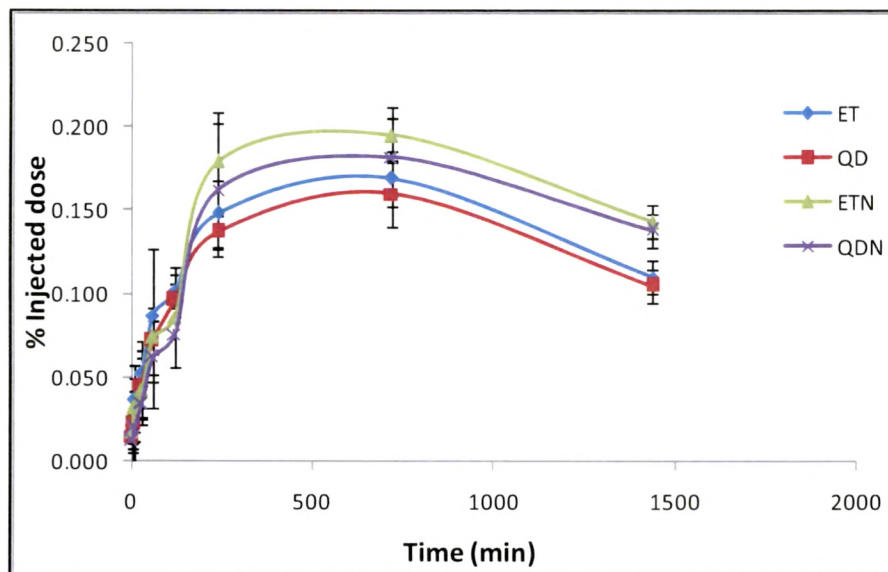
Figure 7.1 % Injected dose of ^{99m}Tc -labeled complexes appearing in blood at various time points

Table 7.4 Biodistribution of ^{99m}Tc -labeled complexes of ET and ETN at 2, 6 and 24 hrs

Organ/ Tissue	% Injected dose per gm of organ (\pm SEM)					
	2 hrs		6 hrs		24 hrs	
	ET	ETN	ET	ETN	ET	ETN
Blood	0.12 \pm 0.02	0.07 \pm 0.01	0.14 \pm 0.03	0.17 \pm 0.02	0.11 \pm 0.01	0.17 \pm 0.02
Heart	0.05 \pm 0.01	0.03 \pm 0.01	0.07 \pm 0.01	0.10 \pm 0.01	0.07 \pm 0.01	0.09 \pm 0.01
Liver	0.21 \pm 0.06	0.23 \pm 0.07	0.34 \pm 0.09	0.50 \pm 0.06	0.22 \pm 0.05	0.23 \pm 0.07
Lungs	0.16 \pm 0.01	0.14 \pm 0.03	0.21 \pm 0.03	0.22 \pm 0.04	0.10 \pm 0.02	0.12 \pm 0.02
Spleen	0.09 \pm 0.08	0.08 \pm 0.01	0.11 \pm 0.03	0.16 \pm 0.08	0.07 \pm 0.01	0.06 \pm 0.01
Kidney	0.33 \pm 0.01	0.21 \pm 0.05	0.72 \pm 0.12	0.53 \pm 0.04	0.18 \pm 0.03	0.22 \pm 0.05
Tumor	0.05 \pm 0.01	0.08 \pm 0.01	0.14 \pm 0.02	0.23 \pm 0.03	0.05 \pm 0.01	0.15 \pm 0.02

n = 3

Table 7.5 Biodistribution of ^{99m}Tc -labelled complexes of QD and QDN at 2, 6 and 24 hrs

Organ/ Tissue	% Injected dose per gm of organ (\pm SEM)					
	2 hrs		6 hrs		24 hrs	
	QD	QDN	QD	QDN	QD	QDN
Blood	0.12 \pm 0.01	0.09 \pm 0.01	0.13 \pm 0.02	0.15 \pm 0.02	0.11 \pm 0.01	0.16 \pm 0.01
Heart	0.06 \pm 0.01	0.04 \pm 0.01	0.06 \pm 0.01	0.09 \pm 0.02	0.06 \pm 0.01	0.09 \pm 0.02
Liver	0.23 \pm 0.07	0.36 \pm 0.06	0.32 \pm 0.08	0.56 \pm 0.09	0.22 \pm 0.04	0.24 \pm 0.06
Lungs	0.18 \pm 0.04	0.16 \pm 0.01	0.27 \pm 0.02	0.21 \pm 0.07	0.11 \pm 0.02	0.12 \pm 0.03
Spleen	0.11 \pm 0.08	0.08 \pm 0.02	0.11 \pm 0.01	0.11 \pm 0.03	0.07 \pm 0.01	0.06 \pm 0.01
Kidney	0.22 \pm 0.01	0.19 \pm 0.03	0.75 \pm 0.05	0.69 \pm 0.12	0.17 \pm 0.02	0.19 \pm 0.05
Tumor	0.04 \pm 0.01	0.07 \pm 0.02	0.09 \pm 0.02	0.20 \pm 0.04	0.04 \pm 0.01	0.13 \pm 0.04

n = 3

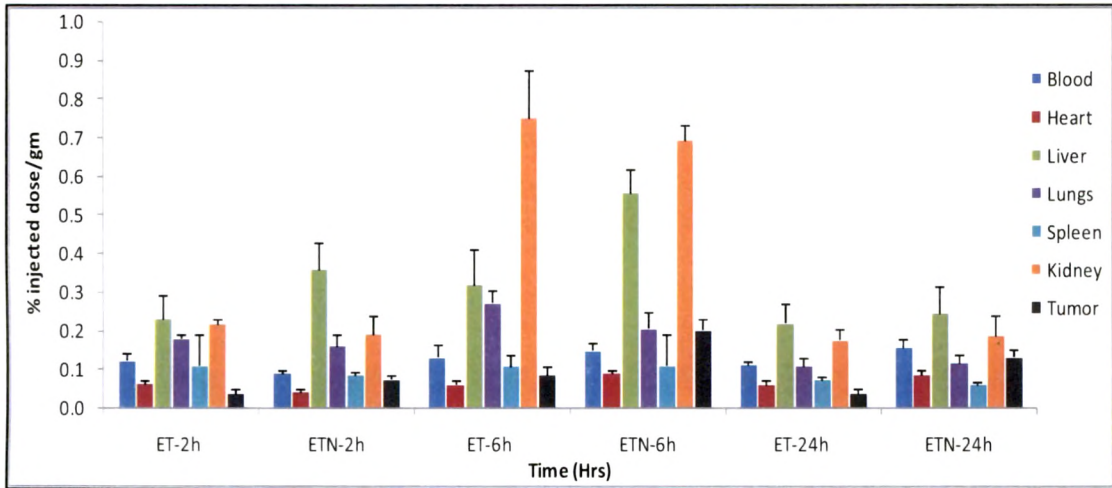


Figure 7.2 Biodistribution of ^{99m}Tc-labelled complexes of ET and ETN at 2, 6 and 24 hrs

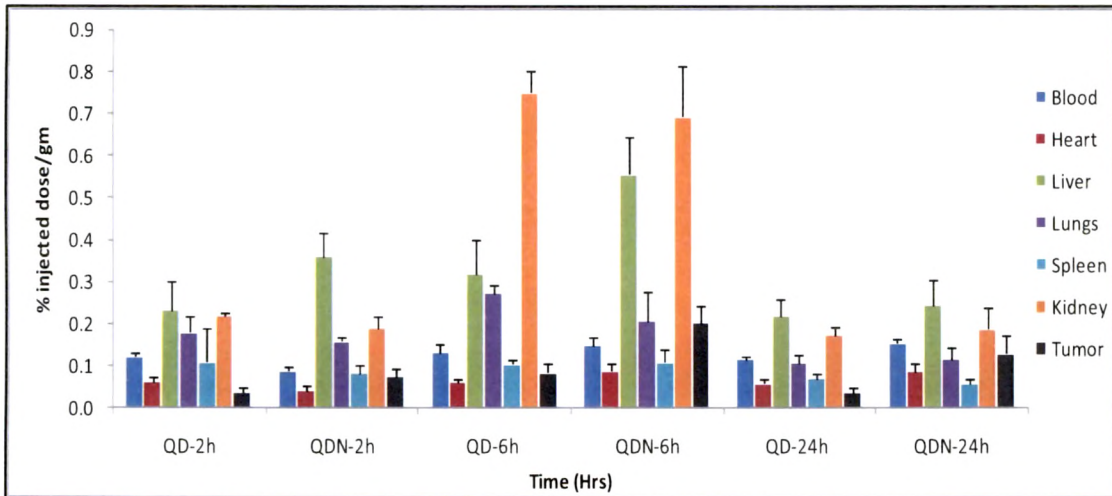


Figure 7.3 Biodistribution of ^{99m}Tc-labelled complexes of QD and QDN at 2, 6 and 24 hrs

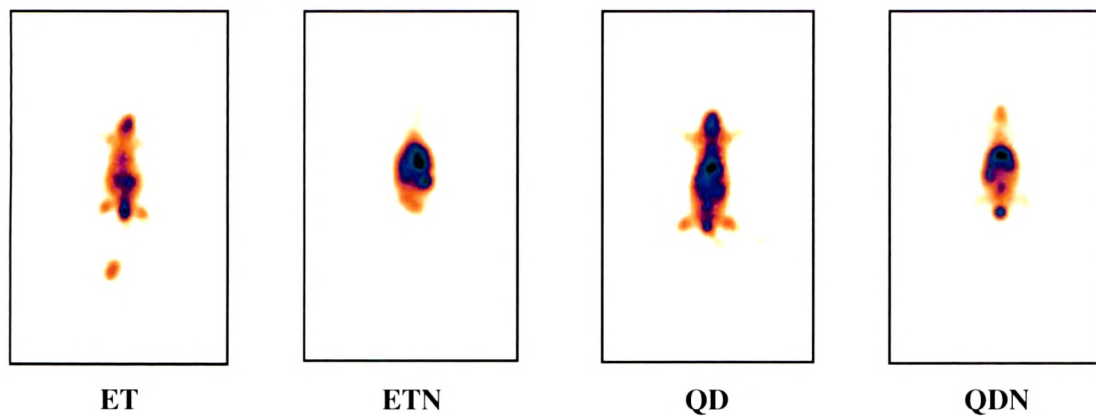
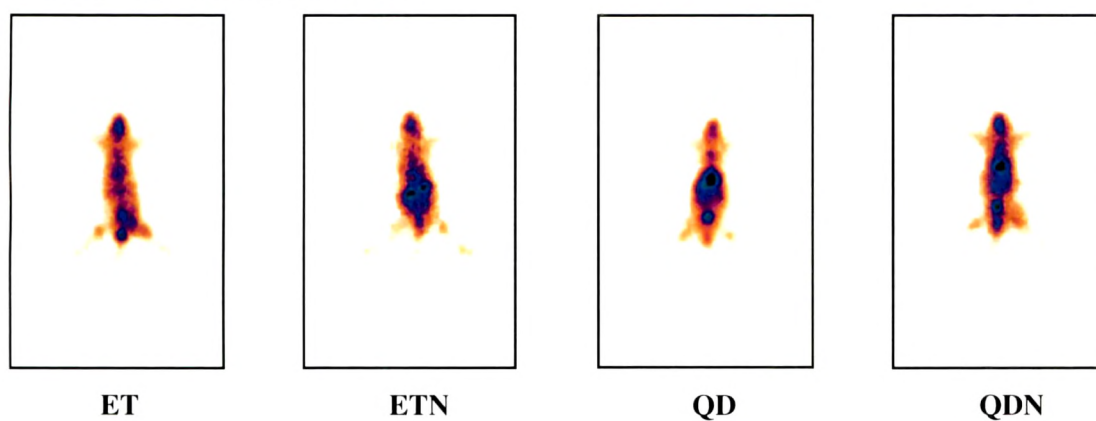
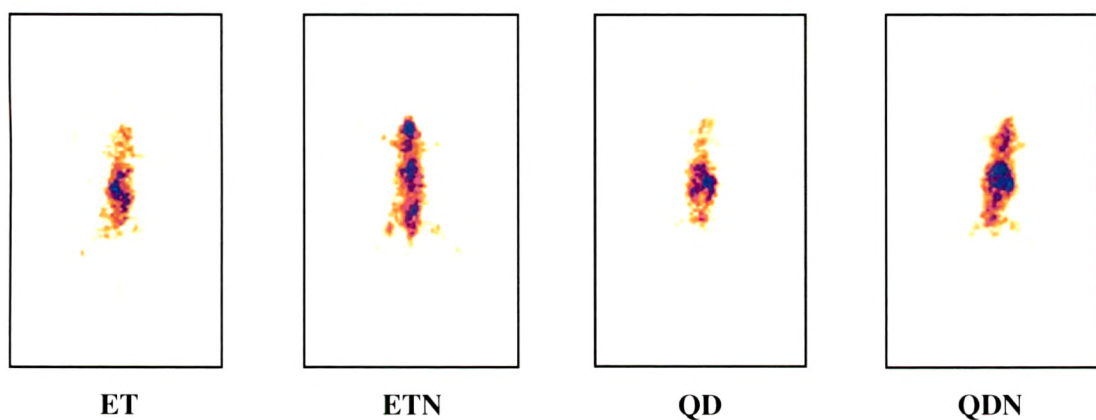
Gamma camera images at 2 hrs.**Gamma camera images at 6 hrs.****Gamma camera images at 24 hrs.**

Figure 7.4 Gamma camera images at 2, 6 and 24 hrs after i.p. injection of ^{99m}Tc -labeled complexes of ET, QD, ETN and QDN

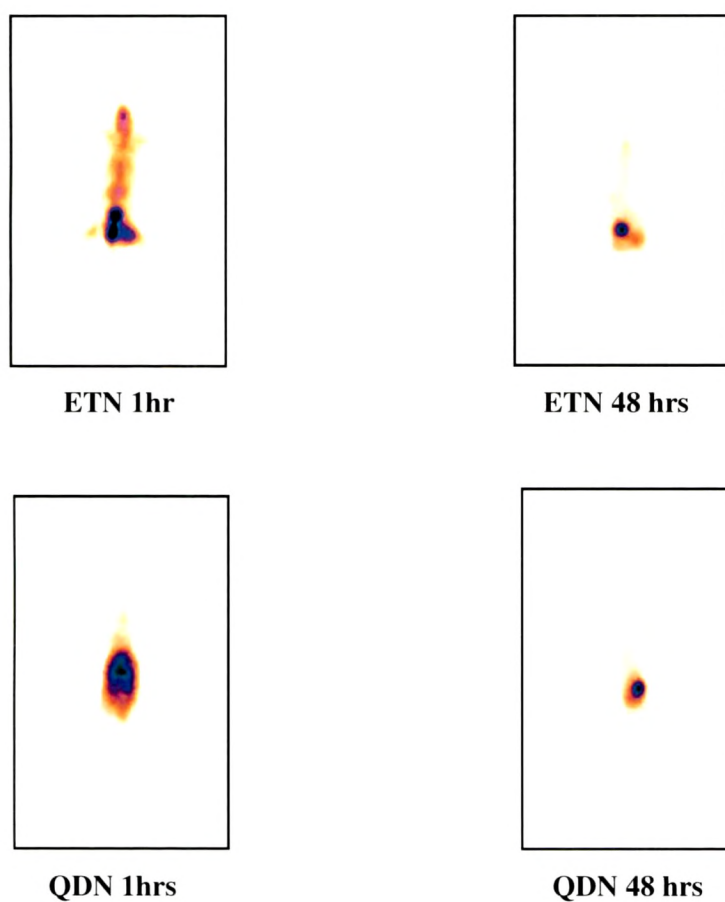


Figure 7.5 Gamma scintigraphy images at 1 hr and 48 hr after s. c. injection near tumor location of ^{99m}Tc -labeled complexes of ETN and QDN

7.3 Tumor growth inhibitory activity:

The use of animals was as per CPCSEA norms and approval for experimental work was as per the local ethical committee of JNCH and RC, Bhopal, India.

Tumor growth inhibitory activity was assessed using B16F10 melanoma model as reported previously (Chen et al., 2005; Sá-Rocha et al., 2006).

B16F16 melanoma tumor induction was carried out according to process previously described in section 7.2.4.

Then animals were coded and randomly divided in nine groups (n = 6 for each group) as control (Untreated), PN (Placebo i.e. drug-free nanoparticles), DMSO (20% aqueous solution), ET, QD, EQ, ETN, QDN and EQN. All animals were housed and fed with standard mouse pellets and water *ad libitum*. All animals were kept at controlled conditions of light (light and dark cycle 12 hrs), temperature $22 \pm 4^\circ\text{C}$ and humidity (45–65%). Treatment was initiated on the first day considering the tumor implantation on zero day. These mice were injected i.p. every third day for 15 days with 2.5mg/kg of ET, 20 mg/kg of QD (in 20% aqueous DMSO) and ETN, QDN (Dispersions in normal saline) equivalent to respective dose of drug (injection volume 0.1-0.15ml). The animals were thus treated with nanoparticle formulations and free drug solutions for single drug as well as for combination of both drugs (in the same dose) in the form of NPs and free drug solutions.

Weights of experimental mice were recorded at regular intervals. Animals with tumor growth delay were observed for their general health condition including body weight.

Tumor diameters were measured every other day with a slide caliper and tumor volume was calculated using the formula:

$$\text{Volume (mm}^3\text{)} = \text{Width}^2 \text{ (mm}^2\text{)} \times \text{Length (mm)} \times 0.52$$

The mice were sacrificed on day 21 to ascertain the size of tumor. The excised tumors were weighed (Table 7.5) and stored in 10% phosphate buffered formalin until further evaluation. Before excision of tumor, the photographs were clicked from a fixed distance to note the angiogenesis process with Sony Cybershot digital camera (Carl Zeiss lens, 7.2 Megapixels)

7.4 Histopathological studies: Tumor microvessel density evaluation

Tumors fixed in 10 % buffered formalin, were processed through a histological routine with a Shandon Pathcentre Tissue Processor. Paraffin sections were cut at 5 μm thickness and stained with hematoxylin and eosin. The slides were observed independently under low-power microscopy (The Nikon microscope, Japan) and the angiogenesis response (tumor microvessel

density) was recorded as 4 (marked), 3 (moderate), 2 (mild), 1 (minimal) and 0 (negative). Comparison of blood vessel density between the control and the different experimental conditions was determined by nonparametric Mann-Whitney rank sum test (Kale et al., 2006). Results are shown in (Table 7.6).

Table 7.6 Effect of various treatments on mean tumor volumes over 21 days period

Days	Mean Tumor Volume (mm ³)								
	Control	PN	DMSO	ET	QD	EQ	ETN	QDN	EQN
0	0	0	0	0	0	0	0	0	0
1	0	0	0	0	0	0	0	0	0
3	0	0	0	0	0	0	0	0	0
5	0	0	0	0	0	0	0	0	0
7	53.24	0	45.03	0	0	0	0	0	0
9	201.61	149.23	122.33	18.68	71.5	0	0	0	0
11	319.48	252.29	298.56	55.8	97.98	0	28.5	65.47	0
13	523.94	533.11	515.22	66.62	178.36	30.71	42.88	83.25	0
15	975.9	718.43	868.66	103.88	353.42	93.63	78.96	242.8	20.66
17	1250.73	1304.22	1280.38	276.16	544.04	186.32	121.99	408.96	58.14
19	1650.62	1585.25	1493.2	444.52	876.53	386.32	250.84	587.4	125.27
21	2043.42	1971.72	1885.37	620.52	989.44	540.38	572.05	874.4	221.05

n= 6

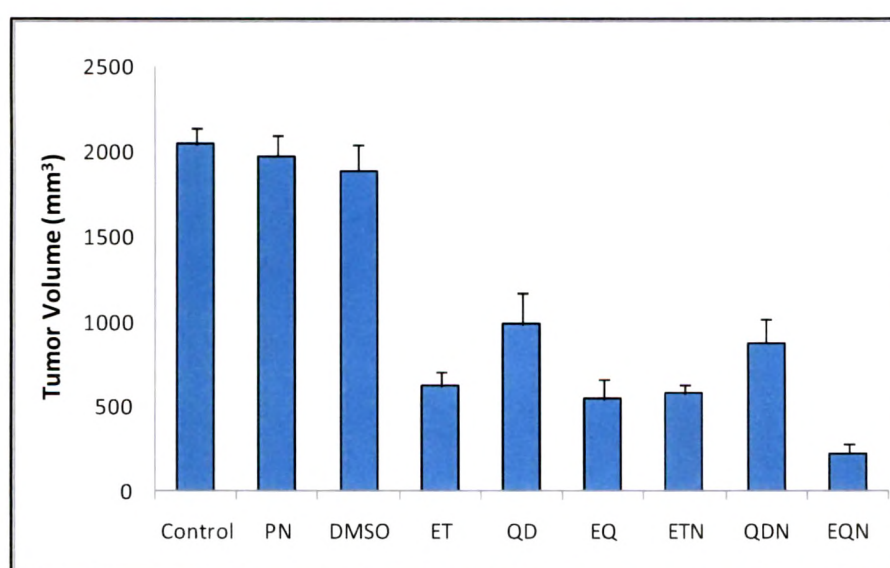


Figure 7.6 Comparison of tumor volumes in response to various treatments on 21st day

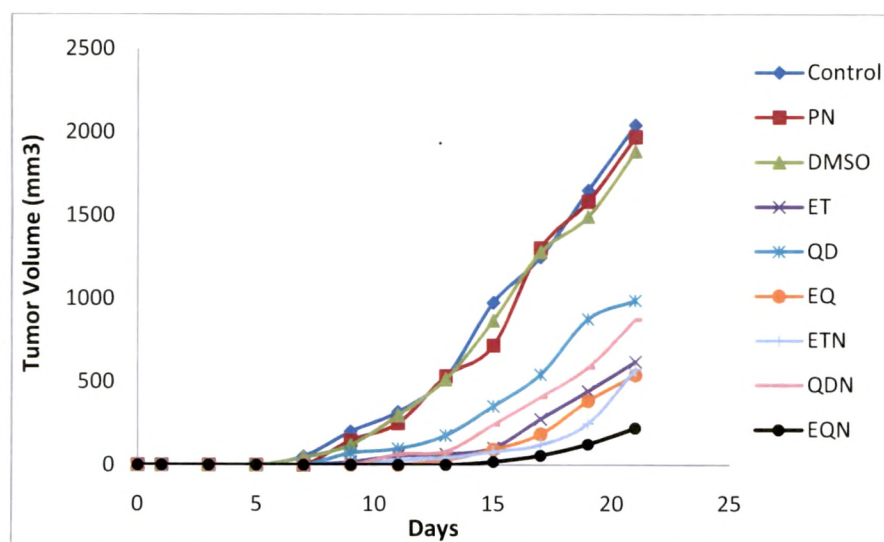


Figure 7.7 Tumor volumes after various treatments to B16F10 melanoma bearing mice

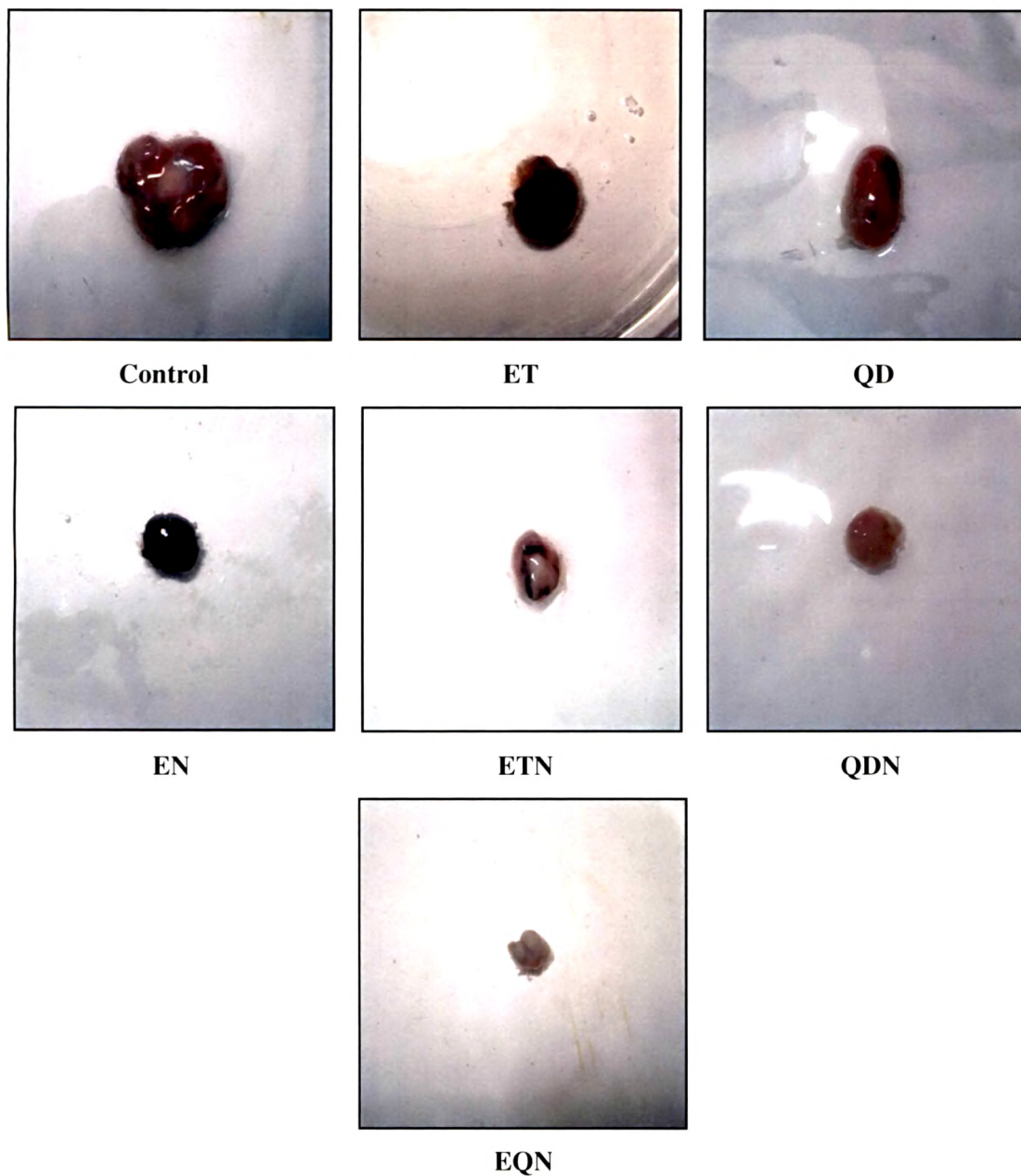


Figure 7.8 Photographs of excised B16F10 melanoma tumors



Control



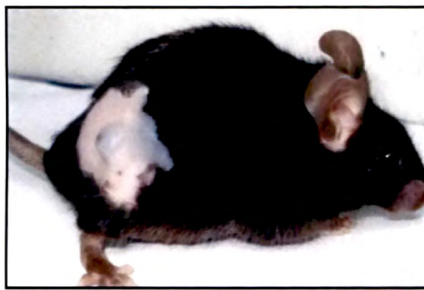
ET



QD



EQ



ETN



QDN



EQN

Figure 7.9 Photographs of B16F10 melanoma bearing mice treated with various treatments

Table 7.7 Effect of various treatments on weight change in B16F10 melanoma bearing mice

Days	Mean weight change in mice (gm)								
	Control	PN	DMSO	ET	QD	EQ	ETN	QDN	EQN
0	0	0	0	0	0	0	0	0	0
1	-1.11	0.12	-0.23	-0.51	-0.45	0.07	-0.15	0.02	-0.09
3	-1.65	-0.77	-0.77	-0.49	-0.57	-0.17	-0.24	-0.81	-1.01
5	-1.55	-1.04	-1.04	-1.27	-0.51	-0.34	-0.33	-0.68	-1.31
7	-0.33	-0.49	-0.68	-1.69	-1.23	-0.5	-0.63	-0.34	-1.07
9	0.27	0.22	-0.21	-1.38	-0.84	-0.62	-0.97	-0.02	-0.99
11	0.61	0.78	0.73	-0.69	-0.11	-0.79	-0.53	0.35	-0.77
13	1.32	1.17	1.38	-0.21	0.53	-0.51	-0.23	0.82	-0.6
15	1.65	1.67	1.66	0.29	1.05	-0.32	0.15	0.98	-0.32
17	2.42	2.21	2.04	0.57	1.52	0.09	0.32	1.23	-0.18
19	3.23	2.87	2.69	0.93	1.88	0.49	0.45	1.46	0.07
21	3.95	3.76	3.34	1.22	2.29	0.87	0.93	1.87	0.32

n = 6

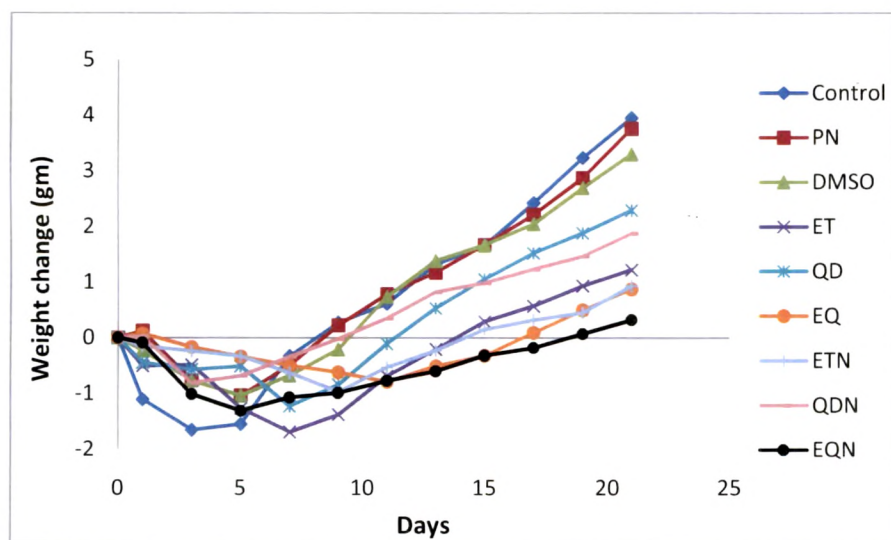


Figure 7.10 Effect various of treatments on weight change in B16F10 melanoma bearing mice

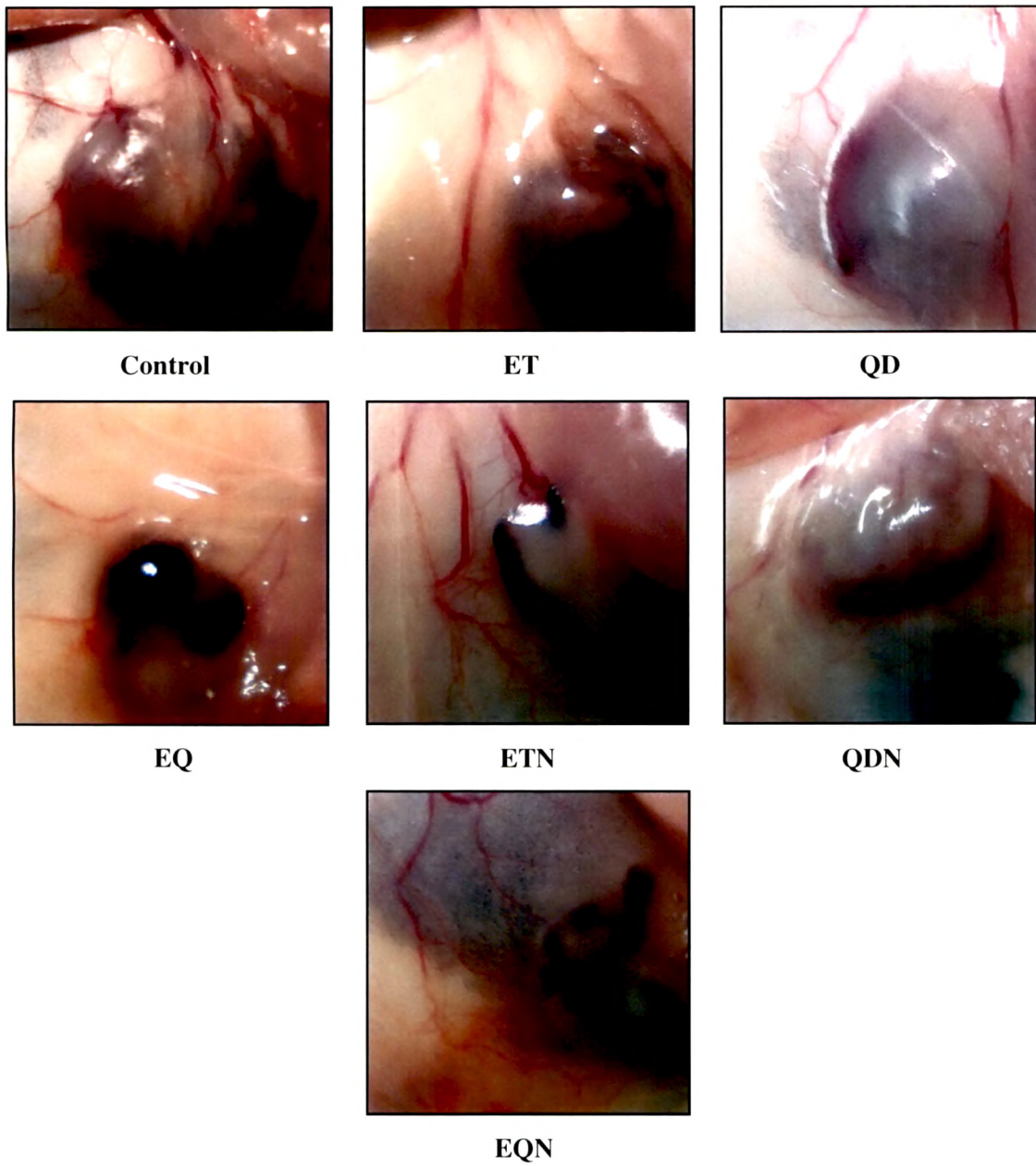


Figure 7.11 Effect of various treatments on angiogenesis on 21st day

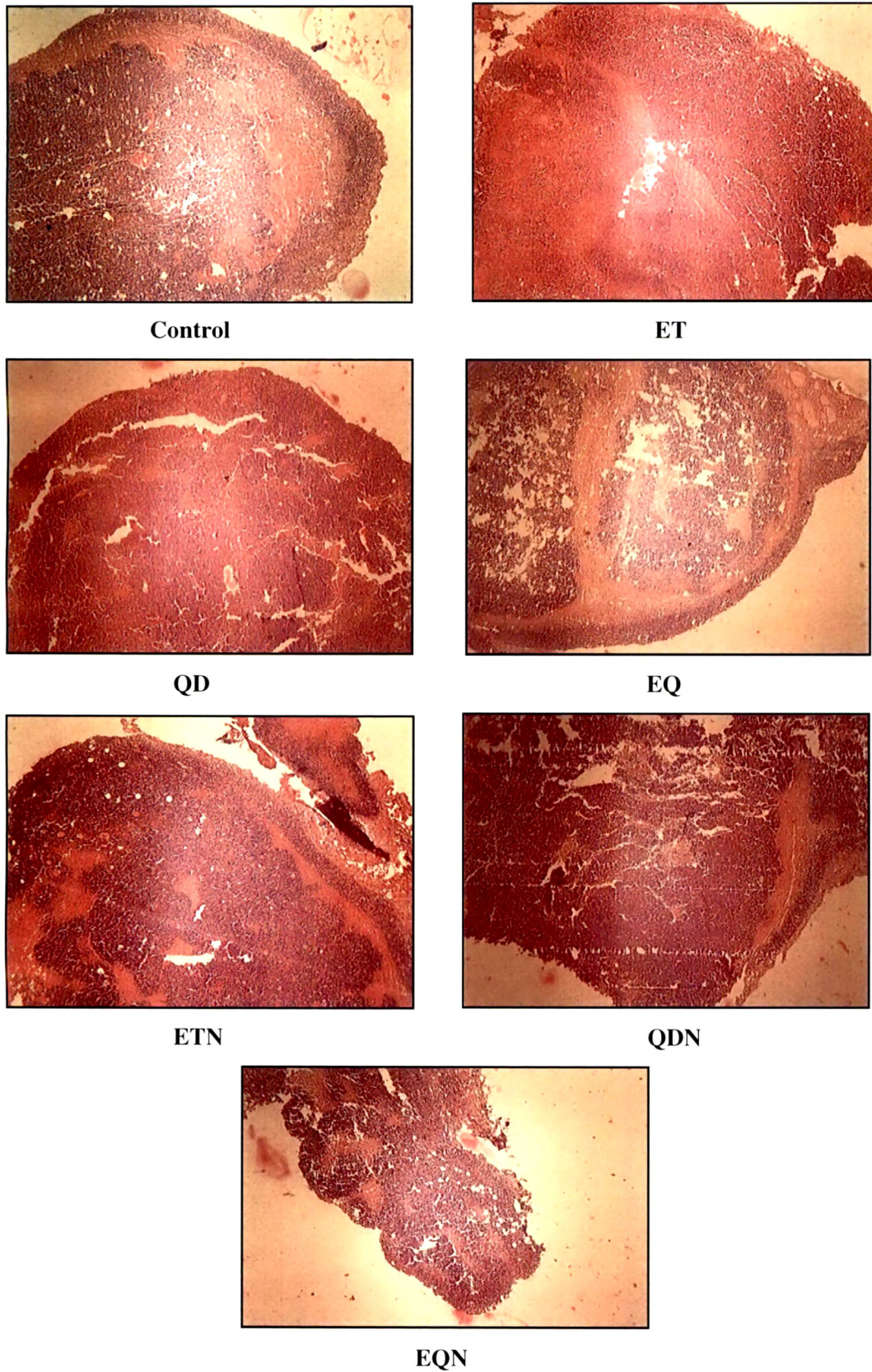


Figure 7.12 Tumor microvessel density (red colored spots) in tumor microsections after staining

Table 7.8 Comparison of degree of angiogenesis for various treatments

Degree of Angiogenesis in various groups									
Animal no.	Control	PN	DMSO	ET	QD	EQ	ETN	QDN	EQN
1	4	3	3	3	3	2	3	2	1
2	4	4	4	3	2	1	2	1	2
3	3	4	4	2	3	3	3	2	1
4	4	3	3	3	1	3	3	1	2
5	3	4	4	4	2	3	3	1	2
6	4	3	4	3	2	2	3	1	1
Rank sum	22	21	22	18	13	14	17	8	9
Z value				3.36	4.16	4	3.52	4.96	4.8

n = 6

7.5 Results and Discussion:

7.5.1 Radiolabeling efficiency:

ET and QD solutions as well as their nanoparticulate formulations ETN and QDN were radiolabeled with ^{99m}Tc with high labelling efficiency which was ascertained by ascending thin layer chromatography. The labelling efficiencies were found to be high for nanoparticulate formulations as compared to the free drug solutions (Table 7.1).

The pertechnetate which exists in heptavalent oxidation state was reduced to lower valence state by stannous chloride. The influence of stannous chloride concentration and incubation time on labelling efficiency is shown in Table 7.1. This optimization is very important because lower amounts of stannous chloride will lead to poor labelling efficiency.

7.5.2 In-vitro serum stability of the ^{99m}Tc -labeled Complexes:

Table 7.2 represents the data of *in vitro* serum stability of ^{99m}Tc labelled complexes of ET, QD, ETN and QDN determined upto 24 hrs. The data demonstrated excellent stability of all complexes in serum except for the ^{99m}Tc -labelled QD solution. It exhibited moderate stability in comparison with the other complexes. Establishing the stability of the labelled complexes in serum is very important as it ensures the strong binding of complex in presence of proteins and many other constituents of serum. The stability of labelled complexes in serum also gives an idea about the stability *in vivo* after administration and their use in determining the biodistribution.

7.5.3 Pharmacokinetic and Biodistribution Study:

Both nanoparticulate formulations ETN and QDN were exhibited higher blood concentrations and extended residence time as compared to ET and QD after 2hrs upto 24hrs. Initially Drug solutions as well as nanoparticulate formulations revealed similar blood concentrations but after 2hrs, the free drug solutions were cleared at a faster rate than ETN and QDN. The respective data and plot of % injected dose appearing in blood Vs time in minutes is shown in Table 7.3 and Figure 7.1. At 1440 min (24hrs), the QD exhibited the lowest concentration among others whereas ETN showed highest concentration. Thus it can be concluded that the nanoparticle delivery system enhances the residence time of drugs in blood.

The biodistribution studies of i.p. injected ^{99m}Tc -labeled complexes of ET, QD, ETN and QDN was performed in C57BL/6 mice. Both free drugs, ET, QD as well as the nanoparticulate formulations, ETN and QDN distributed rapidly to all the organs. At 2 and 6 hrs after injection, no significant difference ($p > 0.01$) in distribution pattern was observed for free drugs and NPs. But free drugs ET and QD exhibited a bit higher concentrations than the corresponding NPs at

2hrs due their faster rate of diffusion (also supported by in- vitro release studies) and at 6 hrs, it became vice-versa.

At 24 hrs, the nanoparticle formulations ETN and QDN showed significantly higher ($p < 0.05$) concentrations than free drugs thus ensuring the prolonged stay of NPs *in vivo* where as free drugs are cleared rapidly.

The tumor uptake of both free drugs ET, QD and nanoparticles ETN, QDN increased with time. The overall tumor uptake of nanoparticles was very significantly higher ($p < 0.01$) than the free drug QD and significantly higher ($p < 0.01$) than ET at 6 and 24hrs (Figure 7.2 and 7.3).

7.5.4 Gamma Scintigraphy:

Figure 7.5 represents the gamma images of B16F10 melanoma tumor bearing mice after subcutaneous injection of ^{99m}Tc -labelled complexes of ETN and QDN taken at 1hr and 48hrs post injection. This study demonstrates the significant tumor uptake and retention. The black and dark blue portions in the figure indicate the melanoma tumor region where the formulations are found concentrated.

7.5.5 Tumor growth inhibitory activity:

Tumor growth in the control, DMSO and placebo treated animals is evident from the data of tumor volumes presented in Table 7.6. This confirms that treatment with either placebo or DMSO did not result in significant changes in tumor volumes. Thus photographs related to groups of placebo and DMSO are not presented in related figures as their results are quiet similar to that produced in Control group.

Treatment with ET and ETN formulation resulted in very signigicant ($p < 0.01$) tumor growth inhibition. The nanoparticulate formulation ETN produced significant ($p < 0.05$) tumor growth inhibition as compared to free form of drug ET, thus underlying the usefulness of the nanoparticle drug delivery system in cancer therapy.

QD and QDN also exhibited significant ($p < 0.01$) tumor growth inhibition. QDN exerted very significant tumor inhibition in comparison with QD. But the tumor inhibition effect produced by QD is significantly ($p < 0.01$) lower than that produced with ET. Hence Quercetin Dihydrate alone, though inhibited tumor growth but did not produce comparable results with chemotherapeutic drug ET. In this study, we used QD as an antiangiogenic drug whose activity is explained later.

The treatment with combination of anticancer and antiangiogenic drugs ET and QD (EQ) produced very significant ($p < 0.01$) tumor growth inhibition as compared with the treatment with any drug alone.

The combination treatment in the form of nanoparticles (EQN) resulted in even higher ($p < 0.05$) tumor inhibition than free drugs combination (EQ) as well as individual drug nanoparticle (ETN /QDN).

By referring to the Table 7.6, it can also be noted that the tumor induction period (Time required to produce the palpable tumor of 50-100 mm³ volume after inoculation of mice with tumor cells) was maximum (16 days) for EQN treatment which is more than double the period that required for the control group (7 days).

The order of tumor growth inhibition activity for various treatments was found as

EQN > EQ > ETN > ET > QDN > QD > Control.

All the statements made above can be clearly depicted in Figures 7.6, 7.7, 7.8 and 7.9.

Figure 7.6 shows the comparison of tumor volumes in response to various treatments on 21st day after tumor inoculation. The minimum mean tumor volume was exhibited by the EQN group amongst all the treatments. It was nearly 10 folds less than the control group (221.05 mm³ for EQN and 2043.42 mm³). Thus with the EQN treatment, life expectancy was supposed to be improved many folds.

Figure 7.7 shows the graph of tumor volumes after various treatments to B16F10 melanoma bearing mice against days (21 days protocol post inoculation).

Figure 7.8 shows the photographs of excised B16F10 melanoma tumors from the various groups.

Figure 7.9 shows the photographs of tumor bearing C57BL/6 mice on 21st day postinoculation of tumor cells.

Table 7.7 depicts the effect of various treatments on weight change in B16F10 melanoma bearing mice. This parameter throw light on the health condition of mice after inoculation with B16F10 melanoma cells and treatment with the chemotherapy as well as combination treatment. A reduction in weight of mice for all groups was observed in initial days of protocol, which is common after inoculation of tumor cells. The weight loss was continued for further as the Control, Placebo and DMSO group developed palpable tumors at 7-8th day and after this the weight of mice was gradually increased due to tumor growth. The ET treatment group led to maximum weight loss of 1.7 gms which is usually observed with chemotherapeutic drugs. The overall health of the mice of this group was observed to be deteriorated in comparison with the other groups. But administering the drug in the form of nanoparticles and adding the

antiangiogenic drug QD to therapy lowered this effect to some extent. This may be attributed to prevention of damage to DNA in normal cells reported by Cierniak et al. (2004).

The positive weight change is minimum for the EQN group while other groups led to higher positive weight change which can be attributed to the higher tumor volumes. Thus it can be concluded that the treatment of mice with the plain drugs resulted in the significant tumor growth inhibition as compared to control. The tumor growth inhibition was further improved when drugs were given in the form of nanoparticles. The combination treatment also showed even better tumor growth inhibition response as compared to single drug treatment. These results are in agreement with those found by Ghosh and Maity (2007)

7.5.6 Histopathological studies:Tumor microvessel density evaluation

Figure 7.11 presents the photographs clicked just prior to excision of tumors. These photographs clearly depict the effect of various treatments on angiogenesis. The control group showed dense or marked microvasculature underlining the role of angiogenesis in the tumor growth. Tumors treated with the QD showed significant reduction in the angiogenesis revealing the QD as potential antiangiogenic agent. Further the antiangiogenesis effect was found significantly improved for the QDN and EQN treatment as compared to plain drug treatments.

These results are supported by the Tumor MVD evaluation (Table 7.8). The Figure 7.12 shows the tumor microsections observed under low power microscopy. The angiogenesis was marked as already described for various treatments and comparison of MVD was made by nonparametric Mann-Whitney rank sum test. The Z-values for QD, QDN and EQN were found as 4.16, 4.96 and 4.8 respectively, thus signifying the role of QD as antiangiogenic agent.

7.6 Conclusions:

The biodistribution studies were successfully carried out and revealed that overall tumor uptake of nanoparticles ETN and QDN is very significantly higher than the free drugs ET and QD at 6 and 24hrs.

The *in-vivo* study, carried out using B16F10 melanoma model (21 days protocol) in C57BL/6 mice enabled us to compare the therapeutic benefit achieved with combination therapy (anticancer drug ET + antiangiogenic agent QD) in the form of PLGA nanoparticles against the effects by any single drug treatment (either in free or nanoparticulate form).

The EQN treatment comes out to be the most efficacious as well as safe treatment for treating solid tumors. Though the significance level for this results is low ($p < 0.01$ for comparison of single drug treatment with combination therapy, $p < 0.05$ for comparison of combination therapy

in free form with NPs), still this study holds promise for future developments. The reason behind this is chemotherapy with anticancer drugs alone produces untoward side effects causing enormous difficulties in leading normal life, whereas the EQN treatment is expected to preserve the quality of life as side effects produced due to chemotherapy are dealt quite efficiently.



REFERENCES

Arulsudar N, Subramanian N, Mishra P, Sharma RK, Murthy RSR. Preparation, Characterization and Biodistribution of ^{99m}Tc -labeled Liposome Encapsulated Cyclosporine. *Journal of Drug Targeting*. **2003**;11:187-196.

Budinger TF. Physical attributes to single photon tomography. *Journal of Nuclear Medicine*. **1980**; 21:579.

Chen JX, Gao Y, Liu JW, Tian YX, Zhao J, Cui XY. Antitumor effects of human ribonuclease inhibitor gene transfected on B16 melanoma cells. *The International Journal of Biochemistry & Cell Biology*. **2005**; 37:1219-1231.

Cierniak A, Papie M, Kapiszewska M. Modulatory effect of quercetin on DNA damage, induced by etoposide in bone marrow cells and on changes in the activity of antioxidant enzymes in rats. *Annales Academiae Medicae Bialostocensis Proceedings*. **2004**; 49(1):167-169.

Claffey KP, Brown LF, Aguilu LF. Expression of vascular permeability factor/vascular endothelial growth factor by melanoma cells increases tumor growth, angiogenesis, and experimental metastasis. *Cancer Res*. **1996**; 56:172-81.

Dabrowska-Iwanicka A, Olszewska D, Jalili A, Makowski M, Grzela T, Marczak M, et al. Augmented antitumor effects of combination therapy with TNP-470 and chemoimmunotherapy in mice. *J Cancer Res Clin Oncol*. **2002**; 128(8):433-42.

Folkman J. What is the role of angiogenesis in metastasis from cutaneous melanoma? *Eur J Cancer Clin Oncol*. **1987**; 23:361-3.

Ghosh S, Maity P. Augmented antitumor effects of combination therapy with VEGF antibody and cisplatin on murine B16F10 melanoma cells. *International Immunopharmacology*. **2007**; 7:1598-1608.

Kale R, Saraf M, Juvekar A and Tayade P. Decreased B16F10 melanoma growth and impaired tumor vascularization in BDF1 mice with quercetin-cyclodextrin binary system. *Journal of Pharmacy and Pharmacology*. **2006**; 58(10):1351-1358.

Kreuter J. Nanoparticles, In: *Colloidal drug delivery systems*. Marcel Dekker, New York, **1994**; pp.219-342.

Reddy LH, Sharma RK, Chuttani K, Mishra AK, Murthy RSR. Etoposide-incorporated Tripalmitin Nanoparticles With Different Surface Charge: Formulation, Characterization, Radiolabeling, and Biodistribution Studies. *The AAPS Journal*. **2004**; Article 23, 6(3):1-10.

Sá-Rocha VM, Sá-Rocha LC, Palermo-Neto J. Variations in behavior, innate immunity and host resistance to B16F10 melanoma growth in mice that present social stable hierarchical ranks. *Physiology & Behavior*. **2006**; 88:108-115.

Seyed JH, Ahmadi A, Taghvai R. Preparation and biodistribution study of technetium- 99m -labeled quercetin as a potential radical scavenging agent. *J Radioanal Nucl Chem*. **2010**; 284:563-566.

Song X, Zhao Y, Hou S, Xu F, Zhao R, He J, Cai Z, Li Y, Chen Q. Dual agents loaded PLGA nanoparticles: Systematic study of particle size and drug entrapment efficiency. *European Journal of Pharmaceutics and Biopharmaceutics*. **2008**; 69:445-453.

Sorensen JA, Phelps ME. In: *Physics in nuclear medicine*. Grune and Stratton, New York, **1980**; 263-344.

Subramanian N, Arulsudar N, Sharma RK, Chuttani K, Mishra AK, Murthy RSR. Radiolabeling, Biodistribution and tumor imaging of stealth liposomes containing methotrexate. *J Alasbimm*. **2003**; 22, Article 6.

Trickler WJ, Nagvekar AA, Dash AK. A novel nanoparticle formulation for sustained paclitaxel delivery. *PharmSciTech*. **2008**; 9(2):486-493.

Wu MS, Robbins JC, Ponpipom MM, Shen TV. Modified in vivo behavior of liposomes containing synthetic glycolipids. *Biochim. Biophys. Acta*. **1981**; 674:19-29.

Yuan ZP, Chen LJ, Fan LY, Tang MH, Yang GL, Yang HS, Du XB, Wang GQ, Yao WX, Zhao XM, Ye B, Wang R, Diao P, Zhang W, Wu HB, Zhao X, Wei YQ. Liposomal quercetin efficiently suppresses growth of solid tumors in murine models. *Clin Cancer Res*. **2006**; 12(10):3193-99.